Exploring ice content on partially saturated frozen soils using dielectric permittivity and bulk electrical conductivity measurements

Yanxin Mao[1], Enrique Romero[1,a] and Antonio Gens[1]
[1] *Division of Geotechnical Engineering and Geosciences, Department of Civil and Environmental Engineering, Universitat Politècnica de Catalunya, 08034, Barcelona, Spain*

Abstract. The present paper explores the use of the measurement of bulk electric conductivity and relative dielectric permittivity during freezing and thawing to estimate the ice content of two different partially saturated soils. The soils (Castelldefels fine sand and Barcelona clayey silt) were prepared at different degrees of saturation and dry densities at room temperature. Different target temperatures were used, which were reached at varying freezing rates and controlled with a thermal bath. Models were used to fit electrical conductivity and relative dielectric permittivity results under full unfrozen liquid and maximum ice conditions. The extension of these models allows estimating ice content on partially saturated soils at different porosities.

1 Introduction

When dealing with the modelling of thermo-hydro-mechanical coupled processes induced by freezing of saturated and unsaturated soils, an important issue is the definition of the freezing retention model, which links the saturation degree of the liquid phase (unfrozen water) to the temperature of the soil. The Clausius-Clapeyron-Poynting equation, which governs the condition for equilibrium between the coexisting liquid water and ice phases, together with a modified form of the van Genuchten equation to take into account the liquid-ice surface tension is usually adopted to represent this freezing retention model. Thus, determining experimentally the amount of ice content or unfrozen water in the frozen soils is necessary and helpful for verifying the correctness of the retention model and also for defining the model parameters.

For the direct measurement of ice content in frozen soil, several methods have been used, including gas dilatometry, dielectric spectroscopy and the heat pulse probe method (see for instance, [1]). Instead of measuring ice content directly, some authors combined two methods together to infer ice content and unfrozen water content in frozen soil [1, 2]. However, it is still difficult to measure the accurate ice content of frozen soil both in direct and indirect way.

The present paper explores ice content on two different partially saturated soils by controlling temperature at different liquid saturations during freezing and thawing process. The soils (a sand and a clayey silt) were prepared at different degrees of saturation and dry densities at room temperature. The technique used to measure the unfrozen liquid saturation was based on frequency domain reflectometry (FDR) measurements, as well as on electrical and thermal conductivity at different target freezing temperatures. These temperatures were reached at varying freezing rates and controlled by a thermal bath. Different models were used to fit electrical conductivity and relative dielectric permittivity results of the partially saturated soils under full unfrozen liquid and maximum ice conditions. These models were then extended for different degrees of unfrozen liquid and ice content, as well as varying porosities. This way, the combination of two methods (electrical conductivity and relative dielectric permittivity results) on a partially saturated soil of known porosity will allow inferring its ice and unfrozen water contents.

2 Description of the models

A simple model was developed by Archie (1942) relating the electrical conductivity of soils to its porosity and saline liquid saturation. For different liquid and ice saturations, the model can be written as (see for instance, [3]):

$$\sigma_{t_l} = a_l^{-1}\sigma_l n^{m_l} S_l^{p_l} \quad \text{and} \quad \sigma_{t_i} = a_i^{-1}\sigma_i n^{m_i} S_i^{p_i} \tag{1}$$

where σ_t denotes the electrical conductivity of the soil, σ represents the electrical conductivity of saline water, S the degree of saturation, n the porosity, m an exponent of the material that can be related to tortuosity or to pore shape and structure, p a saturation exponent and a a tortuosity factor. Subscripts 'l' and 'i' indicate the different phases of

[a] Corresponding author: enrique.romero-morales@upc.edu

the saline water, which are unfrozen liquid water and ice phase respectively.

In unsaturated frozen soils, four phases exist, i.e., soil solids, air, unfrozen water and ice. Because of the large resistance of soil solids and air compared to unfrozen water and ice, they are regarded as insulators. Thus the electrical conductivity can be expressed following an additive way as follows (in accordance to a parallel configuration in which the total current is the sum of the currents through the individual components):

$$\sigma_t = \sigma_{t_l} + \sigma_{t_i} = a_l^{-1}\sigma_l n^{m_l} S_l^{p_l} + a_i^{-1}\sigma_i n^{m_i} S_i^{p_i} \quad (2)$$

For the sake of simplicity, a similar law is adopted for (relative) dielectric permittivity:

$$\varepsilon_t = a_l^{-1}\varepsilon_l n^{m_l} S_l^{p_l} + a_i^{-1}\varepsilon_i n^{m_i} S_i^{p_i} \quad (3)$$

Chen et al. [4] also presented a simplified soil resistivity model to describe the relationships between electrical resistivity, degree of saturation and porosity, which can be expressed for liquid water and ice phases as:

$$\rho_{t_l} = \alpha_l \frac{\rho_l}{S_l n} + c_l \quad \text{and} \quad \rho_{t_i} = \alpha_i \frac{\rho_i}{S_i n} + c_i \quad (4)$$

where ρ_t is the electrical resistivity of the soil, α a structure factor, S the degree of saturation, n the porosity and c a constant. Subscripts 'l' and 'i' indicate the unfrozen liquid or ice phases of the water.

Electrical conductivity σ is defined as the inverse of resistivity. So for a partially saturated soil where unfrozen liquid and ice coexist, the soil electrical conductivity can be expressed as:

$$\sigma_t = \frac{S_l n \sigma_l}{\alpha_l + c_l S_l n \sigma_l} + \frac{S_i n \sigma_i}{\alpha_i + c_i S_i n \sigma_i} \quad (5)$$

For (relative) dielectric permittivity, and for the sake of simplicity, a similar expression to Eq. (5) will be also adopted:

$$\varepsilon_t = \frac{S_l n \varepsilon_l}{\alpha_l + c_l S_l n \varepsilon_l} + \frac{S_i n \varepsilon_i}{\alpha_i + c_i S_i n \varepsilon_i} \quad (6)$$

The unknown model parameters in Eqs. (1) and (4) under full unfrozen liquid $S_i = 0$ and maximum ice $S_l \approx 0$ conditions will be obtained by fitting the experimental curves using a nonlinear least square method. At known porosity, the above equations can be used to estimate ice content in partially saturated frozen soils with $S_l < 1$ and $S_i < 1$, once electrical conductivity and relative dielectric permittivity are known.

3 Materials and experimental methods

3.1 Test materials

Fine sand of Castelldefels (Barcelona) and Barcelona (BCN) clayey silt were studied [5]. The particle size of fine sand varied between 75 and 500 μm. The BCN clayey silt was modified to remove particle sizes larger than 2 mm. The solid densities of sand and clayey silt are ρ_{ss}=2.65 Mg/m^3 and ρ_{sc}=2.67 Mg/m^3, respectively. A 5% NaCl solution (mass basis) was used to perform the freezing-thawing test, and to allow better discriminating between ice and unfrozen liquid when using bulk electrical conductivity.

3.2 Experimental methods

A commercial Frequency Domain Reflectometry (FDR) sensor 5TE was used for measuring bulk electrical conductivity (EC) and (relative) dielectric permittivity [6] according to the scheme depicted in Figure 1. Good contact between the small electrodes and the soils is required for EC measurements. The dielectric constant is measured by using capacitance / frequency domain technology. In order to minimise the effects of salinity, 70 MHz frequency was used to make the 5TE sensor accurate. Two additional thermocouples were used for measuring soil temperature. The FDR sensor and thermocouples were pushed directly into the soil samples, which were contained in a cylindrical plastic container (height 109 mm, diameter 110 mm). The container was immersed into antifreeze liquid inside a thermostatically controlled freezer to conduct the freezing-thawing cycle. The temperature ranged from -20°C to 20°C. The soils with different degrees of saturation and porosities were tested during a freezing-thawing cycle to obtain the values of EC and dielectric permittivity at full liquid state $S_i = 0$ in freezing and thawing points (-3.2°C due to pore water salinity effects) and at maximum ice content $S_l \approx 0$ (-20°C).

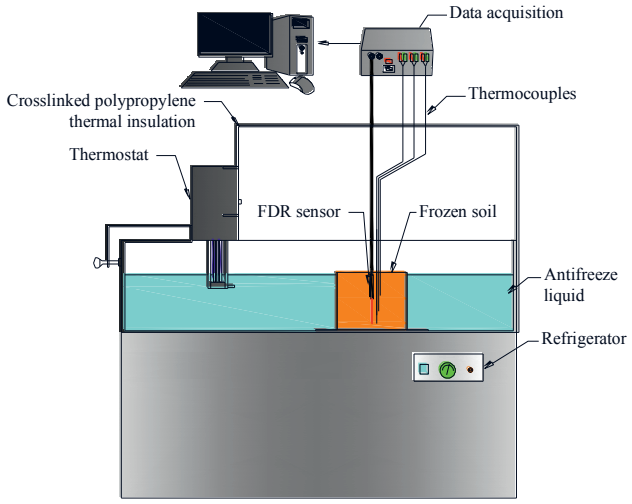

Figure 1. Scheme of the experimental setup.

4 Experimental results and analyses

4.1 Experimental results

Figure 2 shows the time evolution of bulk EC and (relative) dielectric permittivity of a sand sample prepared at $n = 0.49$ and $S_l = 32.9\%$) during a freezing-thawing cycle. It can be observed that the values of bulk EC and dielectric permittivity reduce with decreasing temperature until they reach a minimum, which indicates that the maximum ice condition had been achieved. Similar features were observed during thawing stage (correspondingly, bulk EC and dielectric permittivity increased during this stage). Short plateaus of both bulk EC and dielectric permittivity were observed at the freezing and thawing points.

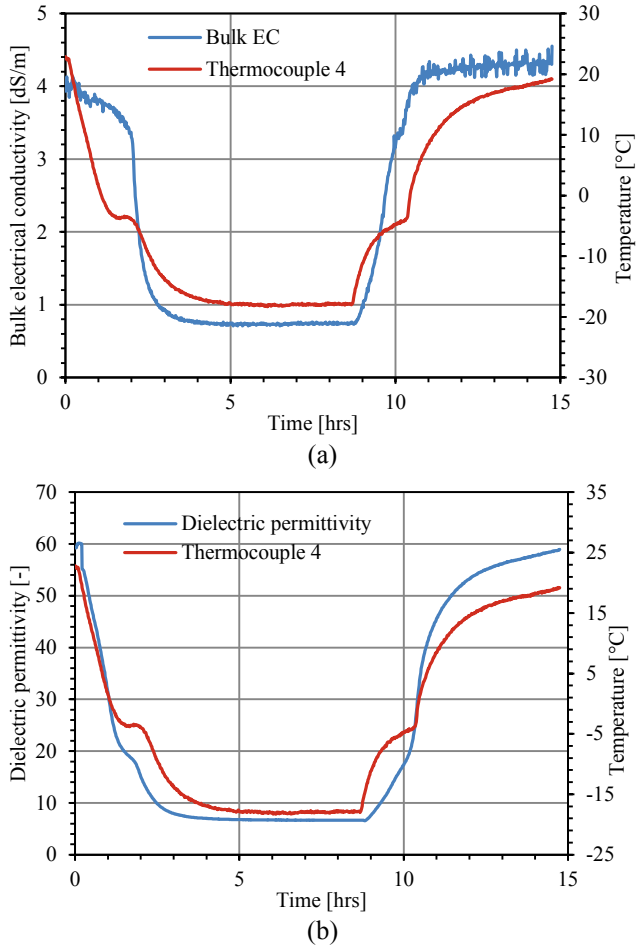

Figure 2. Time evolution of (a) bulk EC; (b) (relative) dielectric permittivity during a freezing-thawing cycle of a sandy sample ($n = 0.49$, $S_l = 32.9\%$).

The variation of bulk EC and (relative) dielectric permittivity with temperature for the two soils are presented in Figure 3. In the relatively dry sand ($n = 0.46$, $S_l = 15.5\%$), the same variation of both bulk EC and permittivity was observed during freezing and thawing. However, in the clayey silt prepared at $n = 0.42$ and $S_l = 47.9\%$, there are some differences in the variation of both bulk EC and dielectric permittivity values between freezing and thawing paths, particularly after the thawing point. Probably this indicates that the soil microstructure (more active due to the wetter state of the clayey silt) has changed during the freezing-thawing cycle.

In total, 15 sand and 12 clayey silt samples have been tested at different values of porosity and degree of saturation, as listed in Table 1. It can be observed that that the porosity of the sand was around $n \approx 0.46$ with major changes in the degree of saturation. This was not the case of the clayey silt, in which the amount of water added affected the fabrication dry density (the porosity changed from 0.32 to 0.52).

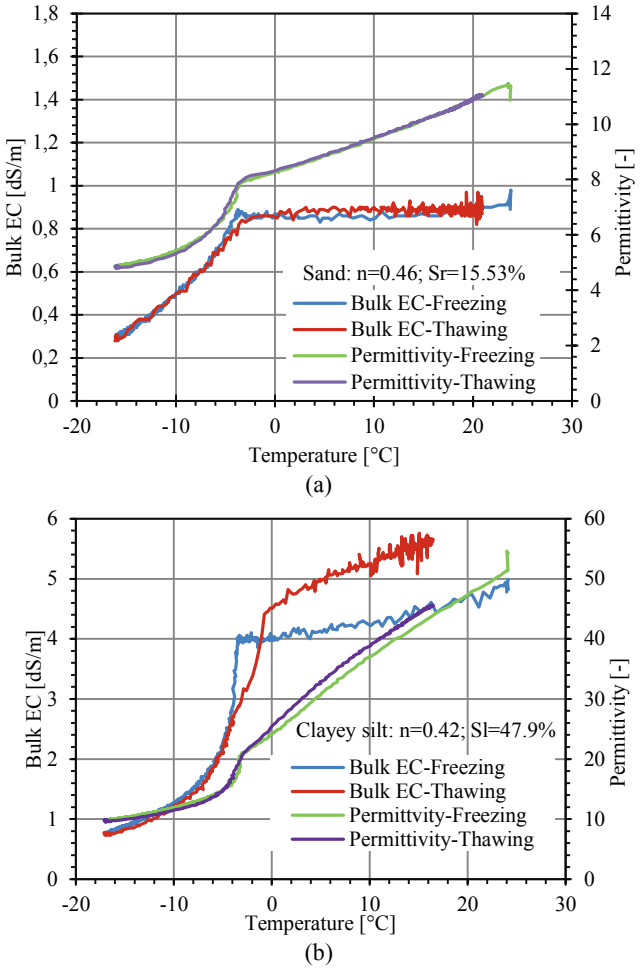

Figure 3. Variation of bulk EC and (relative) dielectric permittivity with temperature during a freezing-thawing cycle: (a) sand; (b) clayey silt.

4.2 Analysis of bulk electrical conductivity results

The bulk EC values of both partially saturated sand and clayey silt samples at maximum ice content $S_l \approx 0$ (-20°C) and at full liquid water state $S_i = 0$ in freezing and thawing point (-3.2°C) are presented in Figure 4. The 'liquid F' and 'liquid T' in the graphs denote the values measured at full unfrozen liquid state during freezing and thawing paths.

Table 1. Initial conditions of soil samples.

Sample	Dry density ρ_d / Mg/m^3	Porosity n / -	Degree of saturation S_l / %
Castelldefels sand			
1	1.43	0.460	15.5
2	1.37	0.483	23.2
3	1.38	0.479	23.9
4	1.36	0.487	32.9
5	1.41	0.468	34.2
6	1.47	0.445	34.9
7	1.40	0.472	36.9
8	1.46	0.449	41.7
9	1.44	0.457	41.7
10	1.40	0.472	43.0
11	1.45	0.453	48.9
12	1.44	0.457	51.7
13	1.47	0.445	57.6
14	1.47	0.445	64.6
15	1.48	0.442	76.0
BCN clayey silt			
16	1.29	0.517	25.7
17	1.41	0.472	35.7
18	1.53	0.427	45.8
19	1.61	0.397	47.1
20	1.53	0.427	47.9
21	1.56	0.416	50.7
22	1.63	0.390	52.0
23	1.70	0.363	56.3
24	1.82	0.318	70.3
25	1.81	0.322	70.3
26	1.79	0.330	79.2
27	1.83	0.315	89.3

Archie's law and Chen's resistivity model have been used to fit the experimental results and thereby to obtain the model parameters. The measured values of bulk EC of pure 5% NaCl solution at maximum ice content (-20°C) and at full unfrozen liquid state (freezing point) were $\sigma_i = 11.7$ dS/m and $\sigma_l = 40.0$ dS/m, respectively. The remaining model parameters can be obtained by fitting the experimental results.

The following two equations can then be used for estimating ice content of partially saturated fine sand from bulk EC readings:

$$\sigma_t = n^{1.6}\left(2.98\sigma_l S_l^{2.0} + 1.74\sigma_i S_i^{1.7}\right) \quad (7)$$

$$\sigma_t = \frac{S_l\, n\, \sigma_l}{1.8 - 0.08 S_l\, n\, \sigma_l} + \frac{S_i\, n\, \sigma_i}{2.4 - 0.32 S_i\, n\, \sigma_i} \quad (8)$$

The equivalent expressions for estimating ice content from bulk EC readings for the clayey silt are:

$$\sigma_t = 1.17\sigma_l n^{1.1} S_l^{2.0} + 0.48\sigma_i n^{1.0} S_i^{1.7} \quad (9)$$

$$\sigma_t = \frac{S_l\, n\, \sigma_l}{3.0 - 0.14 S_l\, n\, \sigma_l} + \frac{S_i\, n\, \sigma_i}{5.0 - 0.67 S_i\, n\, \sigma_i} \quad (10)$$

In Figure 4b the curves have been plotted at constant porosity ($n = 0.46$), whereas the different points display important variations in porosity (this is the reason of the deviations observed at high initial degrees of saturation that were prepared at the denser states).

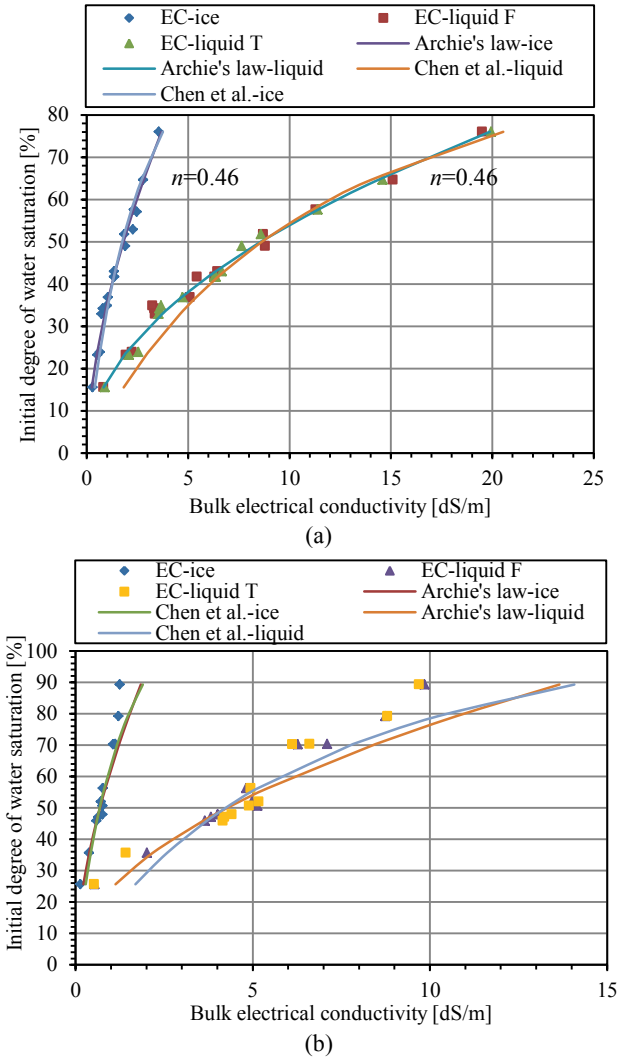

Figure 4. Bulk EC results for different initial degrees of liquid saturation for full unfrozen liquid and maximum ice content: (a) sand; (b) clayey silt.

4.3 Analysis of relative dielectric permittivity results

The (relative) dielectric permittivity values of both sand and clayey silt samples at maximum ice content $S_l \approx 0$ (-20°C) and at full unfrozen liquid state $S_i = 0$ in freezing and thawing point (-3.2°C) are presented in Figure 5. The 'liquid F' and 'liquid T' in the graphs denote the values measured at full unfrozen liquid state during freezing and thawing paths, respectively. The measured values of (relative) dielectric permittivity of pure 5% NaCl solution at maximum ice state (-20°C) and at full unfrozen liquid

state (-3.2°C) were $\varepsilon_i = 66.6$ and $\varepsilon_l = 81.0$, respectively. The value at maximum ice state is very high and can be due to the salinity effect on the FDR measurement. Nevertheless, it has been accepted for fitting purpose (further tests are currently been undertaken to better define the relative dielectric permittivity value at maximum ice state of this reference 5% NaCl solution).

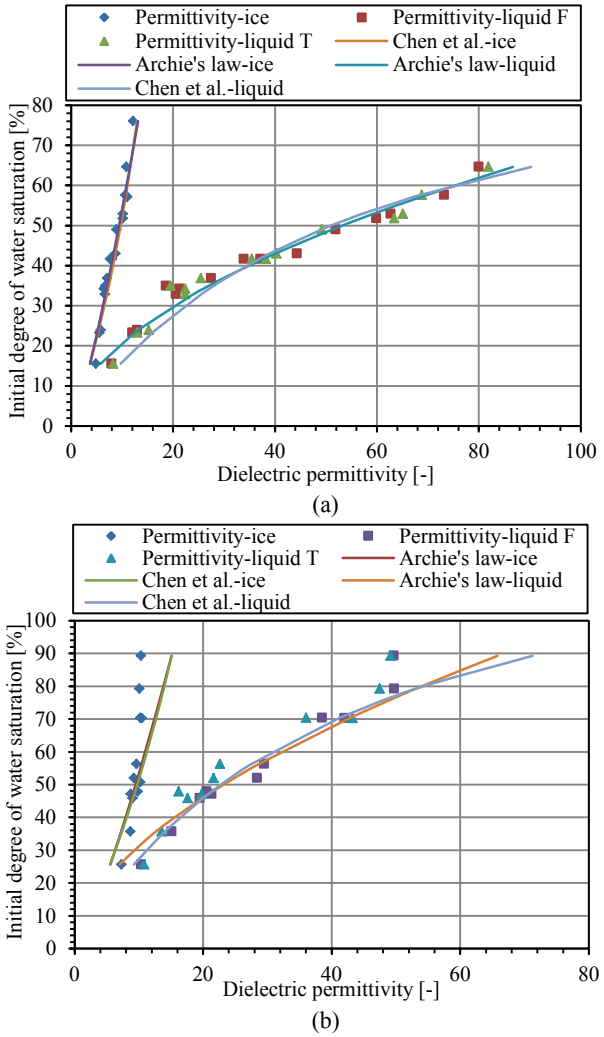

Figure 5. Relative dielectric permittivity results for different initial degrees of liquid saturation for full unfrozen liquid and maximum ice content: (a) sand; (b) clayey silt.

The expressions for estimating ice content in partially saturated sand samples from (relative) dielectric permittivity readings are:

$$\varepsilon_t = 8.50\varepsilon_l n^{1.6} S_l^{1.9} + 0.67\varepsilon_i n^{1.3} S_i^{0.8} \quad (11)$$

$$\varepsilon_t = \frac{S_l\, n\, \varepsilon_l}{0.70 - 0.018 S_l\, n\, \varepsilon_l} + \frac{S_i\, n\, \varepsilon_i}{1.15 + 0.028 S_i\, n\, \varepsilon_i} \quad (12)$$

In the case of the clayey silt, the corresponding expressions are:

$$\varepsilon_t = 1.89\varepsilon_l n^{0.7} S_l^{1.8} + 0.68\varepsilon_i n^{1.1} S_i^{0.8} \quad (13)$$

$$\varepsilon_t = \frac{S_l\, n\, \varepsilon_l}{1.10 - 0.024 S_l\, n\, \varepsilon_l} + \frac{S_i\, n\, \varepsilon_i}{1.10 + 0.020 S_i\, n\, \varepsilon_i} \quad (14)$$

Again, in Figure 5b the curves have been plotted at constant porosity ($n = 0.46$), whereas the different points display important variations in porosity (this is the reason of the deviations observed at high initial degrees of saturation that were prepared at the denser states).

The combination of the two measurements (bulk electrical conductivity and relative dielectric permittivity results) together with the above equations will allow inferring the ice and unfrozen water contents of a partially saturated soil of known porosity.

5 Conclusions

The modified Archie's law and Chen's resistivity model were used to fit the experimental results of both bulk electrical conductivity and relative dielectric permittivity results on two partially saturated soils. The model parameters were determined under full unfrozen liquid $S_i = 0$ and maximum ice content $S_l \approx 0$ conditions. The models were extended to cover intermediate states with $S_l < 1$ and $S_i < 1$. The fitted equations have been proposed for estimating the ice content from bulk electrical conductivity and dielectric permittivity measurements at different porosities and partially saturated states for fine sand and Barcelona clayey silt. It is planned to explore in the future some complementary methods for estimating ice content, involving the determination of specific heat capacity, thermal conductivity and permeability of frozen soils.

Acknowledgements

The first author acknowledges the financial support from China Scholarship Council (CSC).

References

1. X. Zhou, J. Zhou, W. Kinzelbach, F. Stauffer, Simultaneous measurement of unfrozen water content and ice content in frozen soil using gamma ray attenuation and TDR, Water Resour. Res. **50**, 9630–9655 (2014) doi:10.1002/2014WR015640
2. Q. Cheng, Y. Sun, Y. Qin, X. Xue, X. Cai, W. Sheng, Y. Zhao, In situ measuring soil ice content with a combined use of dielectric tube sensor and neutron moisture meter in a common access tube, Agric. Forest Meteorol. **171**, 249–255 (2013)

3. G.E. Archie, The electrical resistivity log as an aid in determining some reservoir characteristics, Transactions of the American Institute of Mining and Metallurgical Engineers **146**, 54-62 (1942)
4. L. Chen, Z. Yin, P. Zhang, Relationship of resistivity with water content and fissures of unsaturated expansive soils, Journal of China University of Mining and Technology, **17** (4), 537-540 (2007) doi:10.1016/S1006-1266(07)60141-2
5. O. E. Cárdenas, R. C. Weber, E. Romero, A. Lloret, J. Suriol, Studying collapse behaviour of sandy silt under generalised stress conditions, Proc. 6th Int. Symposium on Deformation Characteristics of Geomaterials, IOS Press Amsterdam, 462-469 (2015) doi:10.3233/978-1-61499-601-9-462
6. Decagon Devices, Inc, Em50/Em50R/Em50G Em50 Series Data Collection System: Operator's Manual, (2015), http://manuals.decagon.com / Manuals/13453_Em50_Web.pdf.